Available online at www.sciencedirect.com
SCIENCE DIRECT®
Physica D 195 (2004) 29–49
PHYSICA D
www.elsevier.com/locate/physd

Difference equations versus differential equations, a possible equivalence for the Rössler system?

Christophe Letellier[a,*], Saber Elaydi[b], Luis A. Aguirre[c], Aziz Alaoui[d]

[a] *Université de Rouen—CORIA UMR 6614, Av. de l'Université, BP 12, F-76801 Saint-Etienne du Rouvray Cedex, France*
[b] *Department of Mathematics, Trinity University, 715 Stadium Drive, San Antonio, TX 78212-7200, USA*
[c] *Universidade Federal de Minas Gerais, Av. Antonio Carlos 6627, Belo Horizonte 31270-901, Brazil*
[d] *Département de Mathématiques, Université du Havre, BP 540, F-76058 Le Havre Cedex, France*

Received 16 June 2003; received in revised form 16 February 2004; accepted 17 February 2004
Communicated by C.K.R.T. Jones

Abstract

When a set of nonlinear differential equations is investigated, most of time there is no analytical solution and only numerical integration techniques can provide accurate numerical solutions. In a general way the process of numerical integration is the replacement of a set of differential equations with a continuous dependence on the time by a model for which the time variable is discrete. In numerical investigations a fourth-order Runge–Kutta integration scheme is usually sufficient. Nevertheless, sometimes a set of difference equations may be required and, in this case, standard schemes like the forward Euler, backward Euler or central difference schemes are used. The major problem encountered with these schemes is that they offer numerical solutions equivalent to those of the set of differential equations only for sufficiently small integration time steps. In some cases, it may be of interest to obtain difference equations with the same type of solutions as for the differential equations but with significantly large time steps. Nonstandard schemes as introduced by Mickens [Nonstandard Finite Difference Models of Differential Equations, World Scientific, 1994] allow to obtain more robust difference equations. In this paper, using such nonstandard scheme, we propose some difference equations as discrete analogues of the Rössler system for which it is shown that the dynamics is less dependent on the time step size than when a nonstandard scheme is used. In particular, it has been observed that the solutions to the discrete models are topologically equivalent to the solutions to the Rössler system as long as the time step is less than the threshold value associated with the Nyquist criterion.

PACS: 05.45.+b

Keywords: Nonlinear dynamical systems; Discretization; Numerical instabilities; Global modeling

1. Introduction

Until recently, most of the physical processes have been modeled by differential equations where the processes are assumed to be evolving continuously. When these differential equations are nonlinear, there are seldom any

* Corresponding author. Tel.: +33-2-35-146557; fax: +33-2-35-708384.
E-mail address: christophe.letellier@coria.fr (C. Letellier).

0167-2789/$ – see front matter © 2004 Elsevier B.V. All rights reserved.
doi:10.1016/j.physd.2004.02.007

analytical solutions and only numerical integration techniques can provide numerical solutions to the original differential equations. With the advent of digital computers, this is easily done using a fourth-order Runge–Kutta integration scheme. Nevertheless, sometimes it could be desirable to replace the set of continuous-time differential equations with a set of difference equations for which the time is a discrete variable. When standard schemes as the forward Euler, backward Euler or central difference schemes are used, the discrete system has solutions which are equivalent to those of the continuous counterpart only for sufficiently small discretization time steps. With standard scheme, the upper value of the time step for which the solutions are equivalent to the continuous counterpart is significantly smaller than the sampling time used for recording the time evolution of a physical quantity. The question of a possible equivalence between differential and difference equations—with relatively large time steps—and a new scientific theory advocating the discreteness of time have emerged [2,3].

This equivalence is particularly important when comparing different global modeling techniques. Typically, global modeling techniques can be used for obtaining a set of equations that capture the dynamics described by a recorded time series. Such techniques are based on phase space is reconstructions from the measured time series using either delay or derivatives coordinates [4]. If derivative coordinates are used then we obtain a system of ordinary differential equations with dimension equal to the dimension of the original phase space [5]. On the other hand, if delay coordinates are used [6] then a set of difference equations is obtained. Most of time, the dimensions of the obtained models are significantly greater than those of the original systems [7,28]. Such a feature was never considered as a major problem since Takens proposed an existence theorem which ensures the existence of a reconstructed phase space that is diffeomorphically equivalent to the original phase space as long as the dimension of the former is sufficiently large [8]. Indeed, Takens' criterion corresponds to a dimension significantly greater than the dimension of the original phase space. Tempkin and Yorke [9] showed that for almost any choice of measurements (in the sense of prevalence), there exists a scalar difference equation that describes the evolution of the sequence of measurements whose dimension is larger than twice the box-counting dimension of the dynamical system's attractor.

Nevertheless, according to recent works [10–12] where both types of techniques were applied successfully to the same data sets, the dimensions and the number of terms of the obtained global models are different and very much dependent on the techniques used. No direct comparison between the difference and the differential models was therefore possible. Moreover, the obtained global discrete model depends on the discretization time step size [13]. Consequently, it becomes an important task to compare the global models provided by these modeling techniques. It then appears obvious that, before being able to address correctly this problem, it is necessary to have a clear idea of the possible equivalence between differential equations with time step comparable to the sampling time.

For all the above-mentioned reasons, we decided to reinvestigate the possible equivalence between difference and differential equations. This is obviously connected to the important problem of discretizing a set of ordinary differential equations [1,14,15]. In this context, it is well known that the discretization of continuous equations may have solutions which depend on the discretization time step size h and numerical instabilities may be encountered. Numerical instabilities are solutions to the discrete finite difference equations that do not correspond to any solution to the original differential equations. Such a feature occurs mainly when the step size h is too large [16]. This may also be encountered when the order of the difference equations is larger than that of the differential equations [1] which is one way in which models may become overparametrized [17].

A simple example of numerical instabilities is observed in the discretization of the continuous-time logistic map using the Euler scheme. Indeed, the elementary nonlinear ordinary differential equation

$$\dot{x}(t) = x(t)[1 - x(t)] \tag{1}$$

has two fixed points $x_1^* = 0$ and $x_2^* = 1$. The first fixed point is unstable while the second is stable. Thus, every solution of $x(t)$ with $x(0) > 0$ is asymptotically stable. Using the Euler-type discretization scheme

$$\dot{x}_n \approx \frac{x_{n+1} - x_n}{h}, \tag{2}$$

where $h > 0$ denotes the discretization step size and x_n the value of $x(t)$ for $t = nh$. The elementary equation (1) thus becomes

$$x_{n+1} = hx_n \left(1 + \frac{1}{h} - x_n\right), \tag{3}$$

which is a slightly modified version of the logistic map. This difference equation has two fixed points which are still $x_1^* = 0$ and $x_2^* = 1$. Nevertheless, the fixed point x_2^* is stable only for $0 < h < 2$. When the discretization step size h is increased beyond $h = 2$, a period-doubling cascade is observed as well as various chaotic attractors and periodic solutions usually encountered in the logistic map. Consequently, it appears that the discretization of Eq. (1) is only valid, from the asymptotic behavior point of view, for a finite interval of the discretization step size. In fact, Eq. (3) may be rewritten as

$$x_{n+1} = \delta_x x_n + \delta_{x^2} x_n^2, \tag{4}$$

where $\delta_x = h + 1$ and $\delta_{x^2} = -h$. If we take $\delta_x = \lambda$ and $\delta_{x^2} = -\lambda$, we obtain the usual logistic map, where λ is the bifurcation parameter. It appears that the discretization of Eq. (1) leads to a discrete equation which has the same structure as the logistic equation since h and λ are closely related. The discretization time step h may be viewed as the bifurcation parameter of the equation. This will be also observed in the less trivial case of the Rössler system also discussed in this paper.

Indeed, we will take advantage of the chaotic Rössler system when investigating, in a more precise way, the possible equivalence between a set of ordinary differential equations and its discretization. The case of the Rössler system, which is a simple set of three ordinary differential equations with chaotic behavior, will be used because the behavior of such a system allows us to use topological analysis [18] providing a quite accurate characterization of the asymptotic behavior. In a rigorous way, difference and differential equations are said to have the same general solution if and only if $u_n = u(t_n)|_{t=nh}$ for $h > 0$. Here, we will investigate a weaker equivalence in terms of solutions characterized by the same topology in the phase space. Such a topological equivalence will be very helpful to *distinguish displacement in the parameter space from numerical instabilities*. Indeed, when the discretization time step size is varied within a certain range, the solution to the discretization model corresponds to a solution of the continuous counterpart with a displacement in the parameter space.

The rest of the paper is organized as follows. Section 2 briefly describes the topology of two characteristic solutions of the Rössler system. In Section 3, different nonstandard discretization schemes are used and their solutions are investigated versus the discretization time step. A discretization of the analytical model, which is obtained when a single variable is "measured", is proposed and some comments on how it relates to the estimation of models from time series are given. Our conclusions are given in Section 4.

2. Rössler system

Let us start by briefly describing two typical solutions to the Rössler system [19] reading as

$$\dot{x} = -y - z, \qquad \dot{y} = x + ay, \qquad \dot{z} = b + xz - cz, \tag{5}$$

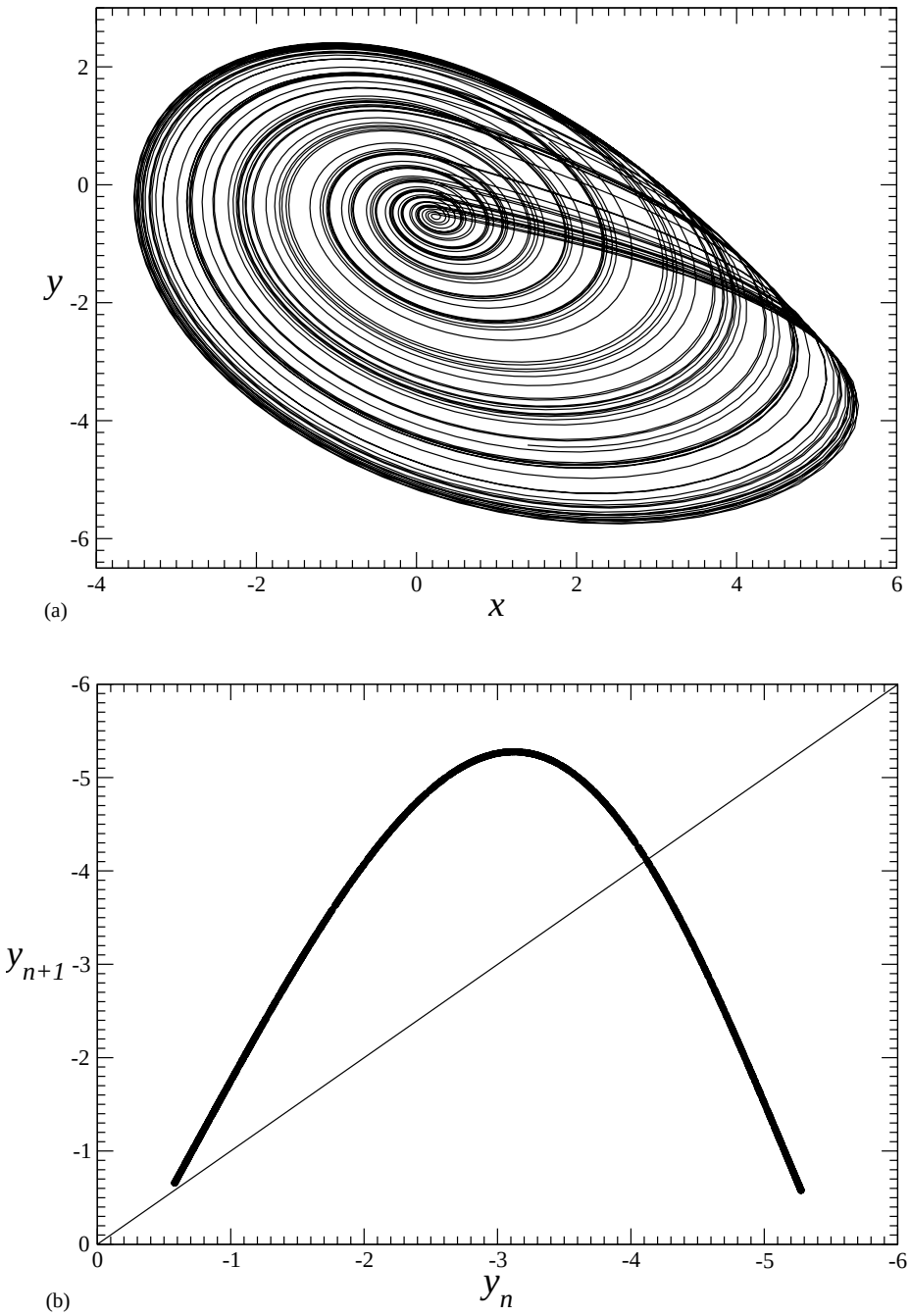

Fig. 1. Spiral attractor generated by the Rössler system (5) with the bifurcation parameters $(a, b, c) = (0.432, 2, 4)$.

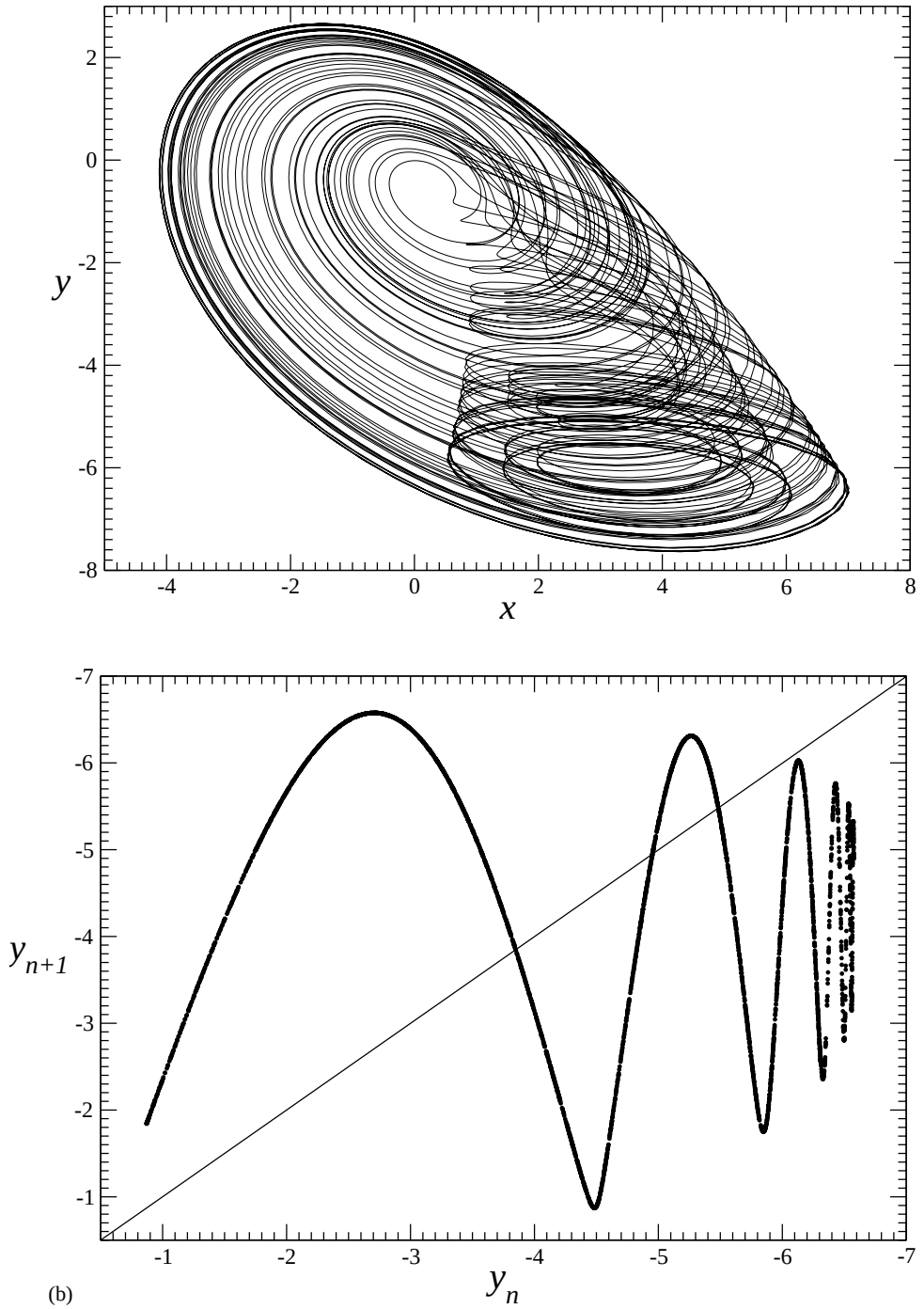

Fig. 2. Funnel attractor generated by the Rössler system (5) with the bifurcation parameters $(a, b, c) = (0.556, 2, 4)$.

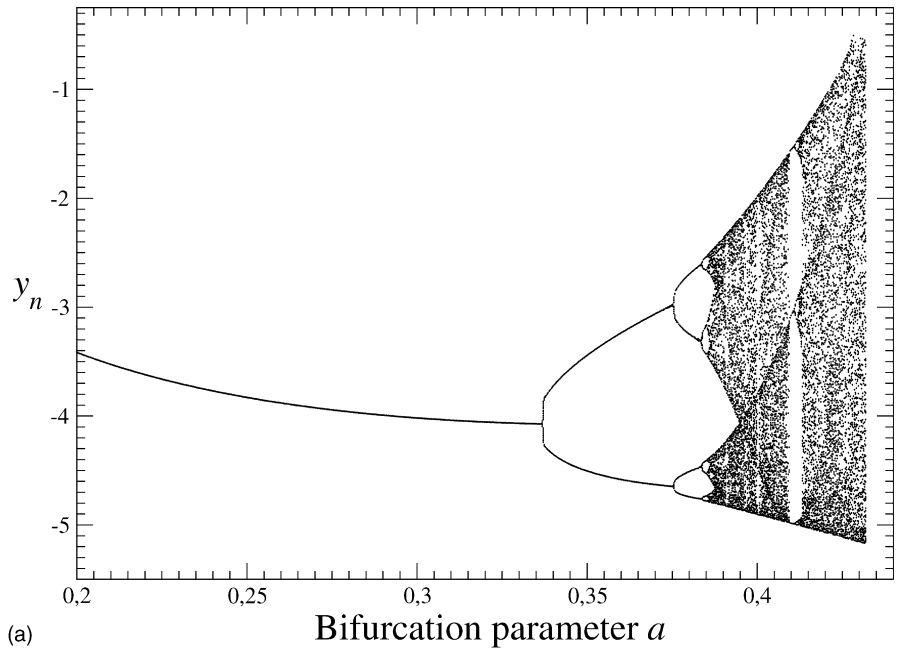

(a)

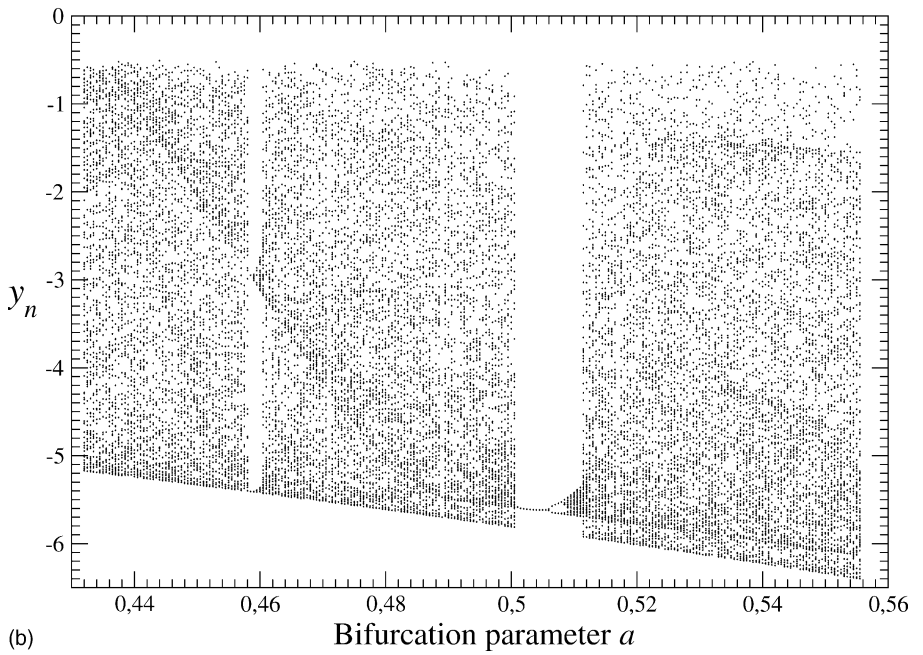

(b)

Fig. 3. Bifurcation diagram vs. the bifurcation parameter a of the Rössler system (5). Part (a) corresponds to values smaller than 0.432 here used as a reference and (b) for values larger than this reference.

where (a, b, c) are the bifurcation parameters. The Rössler system has two fixed points given by

$$x_\pm = \frac{c \pm \sqrt{c^2 - 4ab}}{2}, \qquad y_\pm = -\frac{c \pm \sqrt{c^2 - 4ab}}{2a}, \qquad z_\pm = \frac{c \pm \sqrt{c^2 - 4ab}}{2a}. \tag{6}$$

For $a = 0.432$, $b = 2$ and $c = 4$, the Rössler system has a chaotic attractor for solution (Fig. 1a). According to Farmer et al. [20], we designate this attractor as the *spiral* attractor. This attractor is characterized by a first-return map to the Poincaré section. For three-dimensional systems such a section is defined by the plane

$$P \equiv \{(y_n, z_n) \in \mathbb{R}^2 | x_n = x_-, \dot{x}_n > 0\}, \tag{7}$$

which is unimodal (Fig. 1b). Thus, the map is constituted by an increasing monotonic branch and a decreasing branch separated by the critical point located at the maximum (Fig. 1b). The critical point defines the generating partition of the attractor which allows the encoding of all periodic orbits embedded within the attractor [21]. The increasing branch is close to the bisecting line and, consequently, the symbolic dynamics is almost complete. A two-symbol symbolic dynamics is complete when all periodic orbits which can be encoded with these two symbols are solutions to the Rössler system. Thus, for $a = 0.432$, most of periodic orbits encoded with two symbols are embedded within the attractor generated by the Rössler system.

When the bifurcation parameter a is increased, new periodic orbits are created and the chaotic attractor increases in size (Fig. 2b). The corresponding first-return map is constituted by more than two branches and, for $a = 0.556$, up to eleven monotonous branches may been identified [21]. The corresponding attractor is designated as the *funnel* attractor [20]. For a greater than 0.556, there is metastable chaos, that is the trajectory visits the neighborhood of the unstable periodic orbits solution to the Rössler attractor before being ejected to infinity [21]. The dynamics of the Rössler system can therefore be investigated for $a < 0.556$, b and c remaining constant.

A bifurcation diagram synthesizes the evolution of the dynamics under the change of the bifurcation parameter a (Fig. 3). The bifurcation parameter a is varied over the interval $[0.432, 0.556]$. It will be shown that quite a similar bifurcation diagram is obtained when the discretization time step h of the discretization of the Rössler system is increased.

3. Analytical discretization of continuous systems

3.1. Mickens' guidelines

It is known that discretization of nonlinear differential equations $\dot{\boldsymbol{u}}_i = \boldsymbol{f}_i(\boldsymbol{u}_j)$ may have chaotic behavior while its differential counterpart has a limit cycle or, even just a stable fixed point. Lorenz showed that the discretization version of a simple set of two nonlinear differential equations may exhibit chaotic solutions for sufficiently large values of the discretization time step [22] and Whitehead and Mc Donald showed that the discretization of a two-dimensional nonlinear system can exhibit a chaotic regime [23]. In order to improve the discretization scheme, Mickens formulated a basic set of ad hoc rules for constructing nonstandard schemes for differential equations [24]. We start from the general form

$$\dot{u} \mapsto \frac{u_{k+1} - \Psi u_k}{\varphi}, \tag{8}$$

where Ψ and φ depend on the step size h and other parameters occurring in the differential equations. Functions Ψ and φ should satisfy the conditions

$$\Psi = 1 + \mathrm{O}(h), \qquad \varphi = h + \mathrm{O}(h^2) \tag{9}$$

and may vary from one equation to another. Unfortunately, there is no general way to determine Ψ and φ. In most applications, Ψ is usually selected to be $\Psi = 1$, and φ is determined in such a way that special solutions of the differential equations have the correct stability properties. A general choice for φ may be

$$\varphi_i(h, g_i) = \frac{1 - \mathrm{e}^{-g_i h}}{g_i}, \tag{10}$$

where g_i's are determined as

$$g_i = \max\left(\left|\left.\frac{\partial f_i}{\partial u_i}\right|_{\boldsymbol{u}=\boldsymbol{u}_j}\right|\right), \tag{11}$$

where $\boldsymbol{u}_j$ denote the coordinates of the jth fixed point of the continuous system to discretize.

It is interesting to notice that g_i is related to the the fastest time scale of the system. Therefore, in (10) a normalization is carried out using this fast time scale. The functions φ_i can be interpreted as a "normalized" or a rescaled time step size such that its value is never larger than the smallest time scale of the system. Since many of the mechanisms that lead to the occurrence of numerical instabilities have their origin in using a step size that is greater than some relevant physical time scale, this method for selecting φ_i's reduces this source of instabilities. In other words, the use of functions φ_i, rather than just h, allows the value of h to be much larger than the one normally selected because it is the effective step size φ_i that determines the stability and not the actual step size h. Another issue of great importance is that, in general, nonlinear terms are modeled by discrete expressions that are nonlocal on the computational grid [24]. For instance, a u^2 term would be replaced by $u_{k+1}u_k$ in the finite difference scheme, whereas conventional methods would use the local form u_k^2. An important rule to build discretization schemes is that the order of the discrete equations should be equal to the order of the corresponding derivatives of the differential equations, otherwise spurious solutions (numerical instabilities) may occur [1].

The fundamental reason for the existence of numerical instabilities is that discrete models obtained by discretizing differential equations have parameter spaces with higher dimensions than those of the corresponding differential equations. This is easily argued by the fact that the time step size h can be regarded as an additional parameter. Even if $\{y(\cdot, \lambda)\}$ and $\{y_k(\lambda, h)\}$ are "close" to each other for a particular value of h, say $h = h_1$, if h is changed to a new value, say $h = h_2$, the possibility exists that $y_k(\lambda, h_2)$ differs greatly from $y_k(\lambda, h_1)$ both qualitatively and quantitatively [1].

Our aim is to show how this type of discretization scheme may influence the quality of the discretized model and its sensitivity to the choice of the discretization time step size h. We will investigate three different discretizations. The last one follows all of Mickens' recommendations.

3.2. One simple example

The first discrete model is obtained using the following transformation on system (5):

$$x \mapsto x_k, \qquad y \mapsto y_k, \qquad z \mapsto z_k, \qquad xz \mapsto x_k z_{k+1}. \tag{12}$$

Thus, by applying the discretization scheme (8) with $\Psi = 1$, we obtain the model:

$$x_{k+1} = x_k - \varphi_1(y_k + z_k), \qquad y_{k+1} = (1 + a\varphi_2)y_k + \varphi_2 x_k, \qquad z_{k+1} = \frac{z_k(1 - c\varphi_3) + b\varphi_3}{1 - \varphi_3 x_k}, \tag{13}$$

where the functions are chosen according to

$$\varphi_1 = \varphi_2 = \varphi_3 = \sin h. \tag{14}$$

Although the φ functions could be chosen according to (10), for the sake of simplicity, in this example, they were chosen as shown in (14).

It should be noticed that introducing the nonlocal term $x_k z_{k+1}$ induces the rational form of the third equation. Depending on the choice of the functions φ_i, the discretization of the Rössler system may be stable over a wider interval of the discretization time step h as discussed below.

For a very small discretization time step h, the dynamics underlying the difference equations (13) with φ defined by relation (14) is topologically equivalent to the dynamics of the Rössler system (5). This means that the phase portrait (Fig. 4a) solution of the difference equations (13) with φ_i's defined by relation (14) is also characterized by a first-return map to a Poincaré section (Fig. 4b) equivalent to the one associated with the Rössler dynamics (Fig. 1b). The populations of periodic orbits embedded within the attractors solution of the Rössler system and its discretization are the same. Moreover, both attractors are characterized by the same template, that is, periodic orbits have the same relative organization in the phase space. In other words, the relative organization of periodic orbits may be described by the same branched manifold.

Nevertheless, when the discretization time step h is increased, bifurcations occur and new periodic orbits are created or destroyed. For larger values of h, the first-return map presents new monotonous branches (Fig. 5b) as observed on the Rössler attractor of the funnel type (Fig. 2b). This means that the discretization time step h that functions as a bifurcation parameter, plays the same role as the parameter a does for the Rössler system. Indeed, when h is varied over the range (0.0, 0.0924), the bifurcation diagram (Fig. 6) is rather similar to the one computed versus the a parameter for the Rössler system (Fig. 3b). This discretization of the Rössler system has a chaotic attractor that is topologically equivalent to one solution to its continuous counterpart but with different bifurcation parameter values as long as the discretization time step is sufficiently small. Consequently, the discretized version of the Rössler system remains valid for quite large values of the time step h. Varying the value of the time step h associated to the discrete model, therefore, corresponds to a displacement in the parameter space of the original Rössler system.

Note that the time step cannot be varied over a very large range. In fact, the interval is restricted to a limited range because for values beyond 0.0924 s, the trajectory is ejected to infinity as was observed when parameter a is varied.

Such a modification of the dynamics through the discretization procedure is a common feature observed in global modeling. Indeed, very often the global model estimated from experimental time series does not exhibit exactly the same behavior than the experimental one. This does not mean that the model is bad since, very often, a parameter of the model may be slightly varied to recover the expected dynamics [25]. In other words, for a given value of the time step h, it is possible to modify the bifurcation parameters in order to recover the expected dynamics. For instance, with $h = 0.0924$ s and $a = 0.321$, a two branch first-return map is obtained. In that case, the development of the dynamics induced by the increase of the discretization time step h is canceled out by the decrease of the a parameter. This feature results directly from the coefficient $1 + a\varphi_2$ in the second equation (13) since it is the coefficient of the autoregressive part of the equation. The term $1 + a\varphi_2$ therefore defines the overall dynamics, the second term $\varphi_2 x_k$ being only the forcing function (the exogenous part of the equation). Since $\varphi_2 = \sin h$, the increase of h has to be followed by the decrease of a in order to keep the coefficient $1 + a\varphi_2$ approximately unchanged, and therefore the dynamics of the second equation of (13) constant. Of course, the dynamics of the whole system (13) depends on other things but the compensating effect of a over h is partially explained by this remark.

3.3. An optimized finite difference model

In discrete model (13), we used the nonlocal nonlinear term $x_k z_{k+1}$. It is also possible to choose the other form $x_{k+1} z_k$. In this case, the third equations becomes polynomial

$$z_{k+1} = b\varphi_3 + [1 + \varphi_3(x_{k+1} - c)]z_k \tag{15}$$

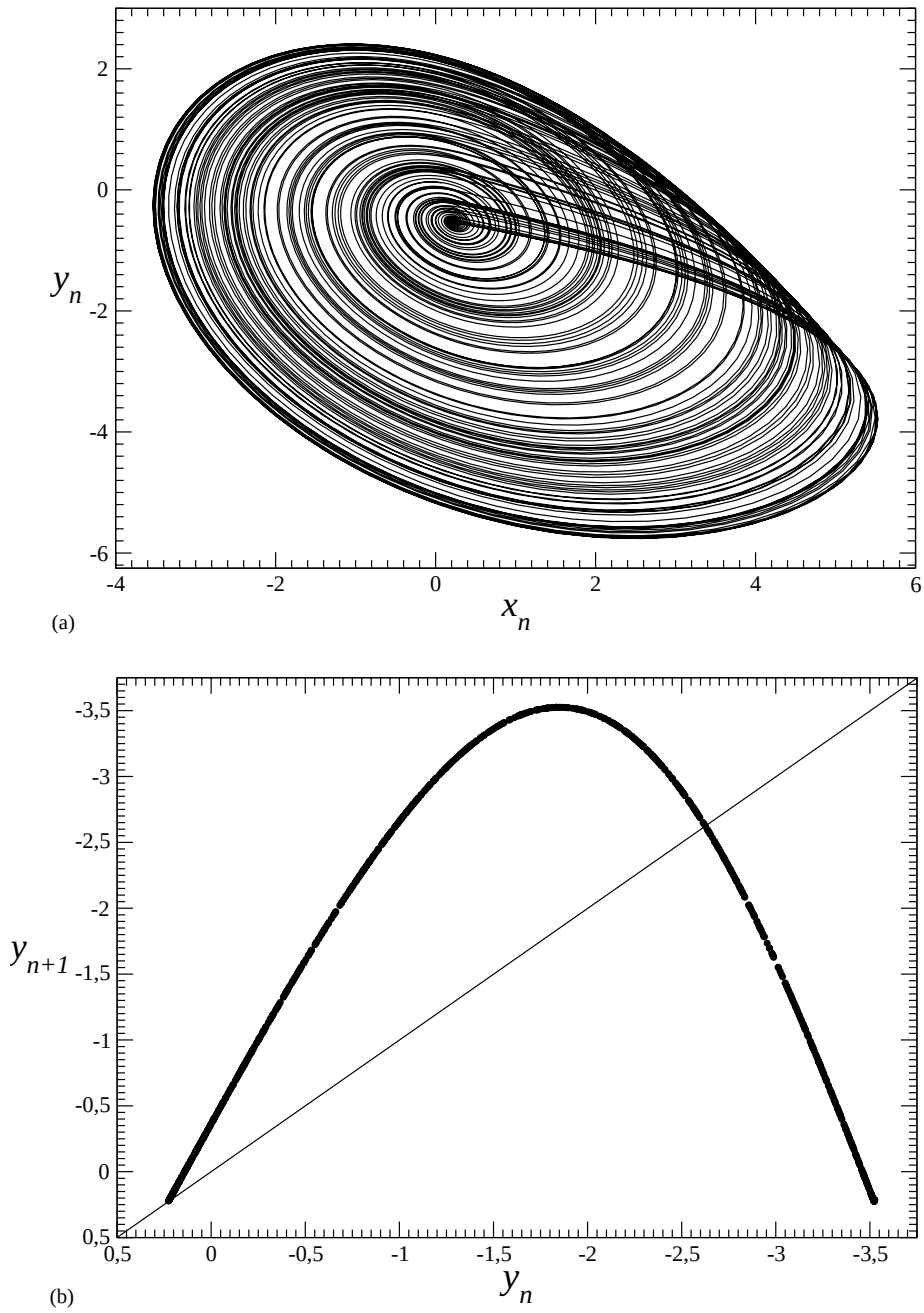

Fig. 4. Spiral chaotic attractor solution of the difference model (13) for the time step $h = 0.001$ s with the functions φ_i given in relation (14).

and the time step can be increased to 0.2405 s which is 2.5 times greater than the upper value reached with discretized model (13). The bifurcation diagram thus obtained is similar to the bifurcation diagram shown in Fig. 6, but with a rescaling of the a-axis between 0 and 0.2405 s.

A more robust discrete model is obtained when we follow all the recommendation given by Mickens for constructing new finite difference equations corresponding to the Rössler system. We use the following transformation:

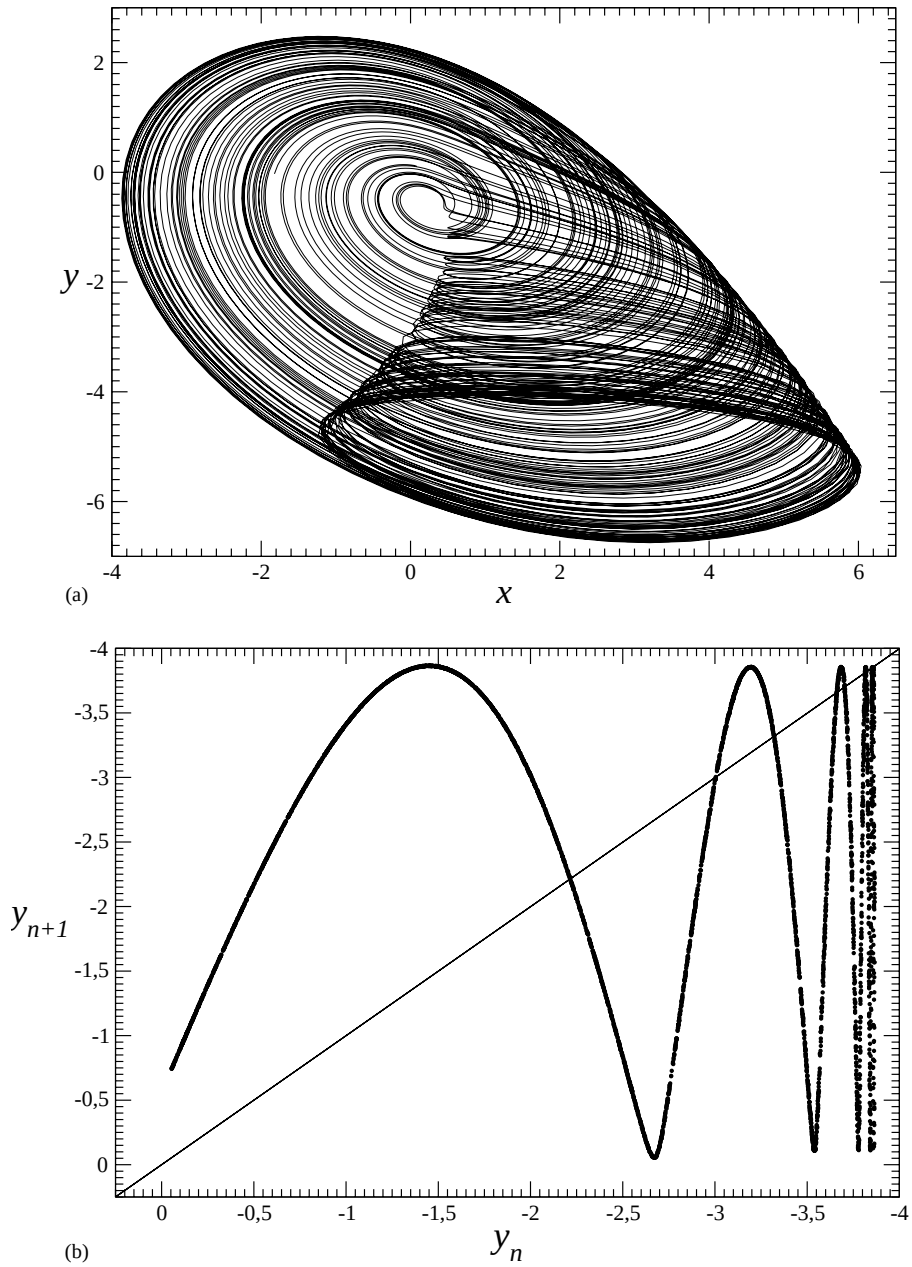

Fig. 5. Funnel chaotic attractor solution of the difference model (13) for the time step $h = 0.0924$ s with the functions φ_i given in relation (14).

- first equation: $(x_k, y_k, z_k) \mapsto (x_k, y_k, z_k)$;
- second equation: $(x_k, y_k, z_k) \mapsto (x_{k+1}, y_k, z_k)$;
- third equation: $(x_k, y_k, z_k) \mapsto (x_{k+1}, y_{k+1}, z_k)$.

and the nonlinearity xz is replaced by the nonlocal term $x_{k+1}z_k$. This choice has also the advantage of preserving a polynomial form for the discretization model. Function Ψ is equal to 1. Thus, we obtain

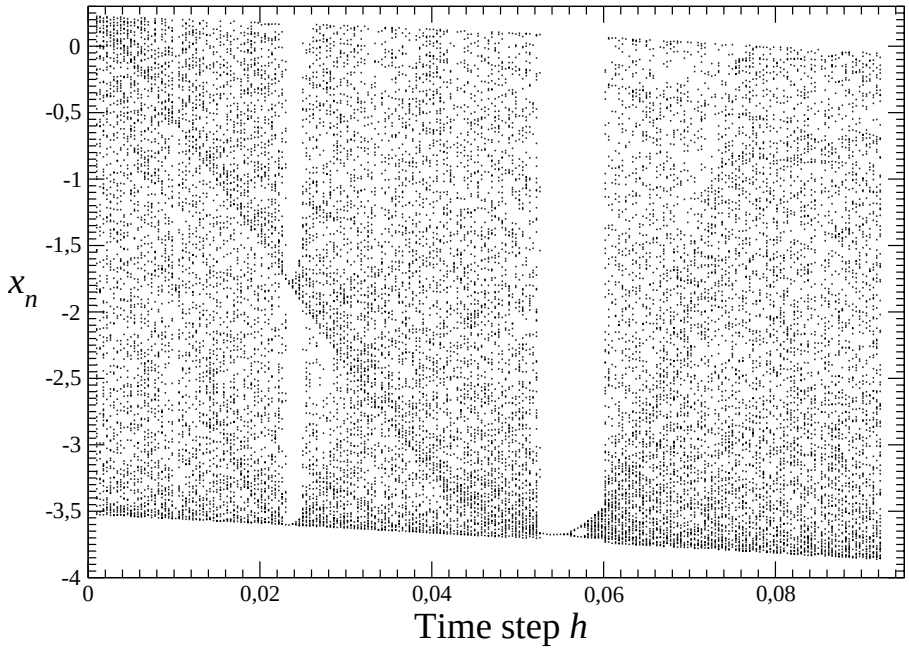

Fig. 6. Bifurcation diagram vs. the time step h for model (13) with the functions φ_i given in relation (14). Compare with Fig. 3b.

$$x_{k+1} = x_k - \varphi_1(y_k + z_k), \qquad y_{k+1} = (1 + a\varphi_2)y_k + \varphi_2 x_{k+1}, \qquad z_{k+1} = b\varphi_3 + [1 + \varphi_3(x_{k+1} - c)]z_k. \tag{16}$$

The function φ_i is chosen according to the on-diagonal elements of the Jacobian matrix of the original continuous system (5):

$$J_{ij} = \begin{bmatrix} 0 & -1 & -1 \\ 1 & a & 0 \\ z & 0 & x - c \end{bmatrix}. \tag{17}$$

Note that since $J_{11} = 0$, there is no natural time scale associated with the autoregressive part of the first equation. We therefore choose the function φ_1 equal to h, thus expressing this fact. According to Eqs. (10) and (11), the second function is

$$\varphi_2 = \frac{1 - \mathrm{e}^{-ah}}{a} \tag{18}$$

and the third one is

$$\varphi_3 = \frac{1 - \mathrm{e}^{-x_c h}}{x_c}, \tag{19}$$

where $x_c = (-c + \sqrt{c^2 - 4ab})/2$ is estimated using the fixed point coordinates and Eq. (11). Note that the optimized model (16) is polynomial.

This discrete model can be iterated with a discretization time step size h over the range (0, 0.6194), that is over three times larger than the one used with the previous discretization schemes. The bifurcation diagram versus h (Fig. 7) is similar to the diagrams computed with the continuous Rössler system (Fig. 3) if the a parameter is varied

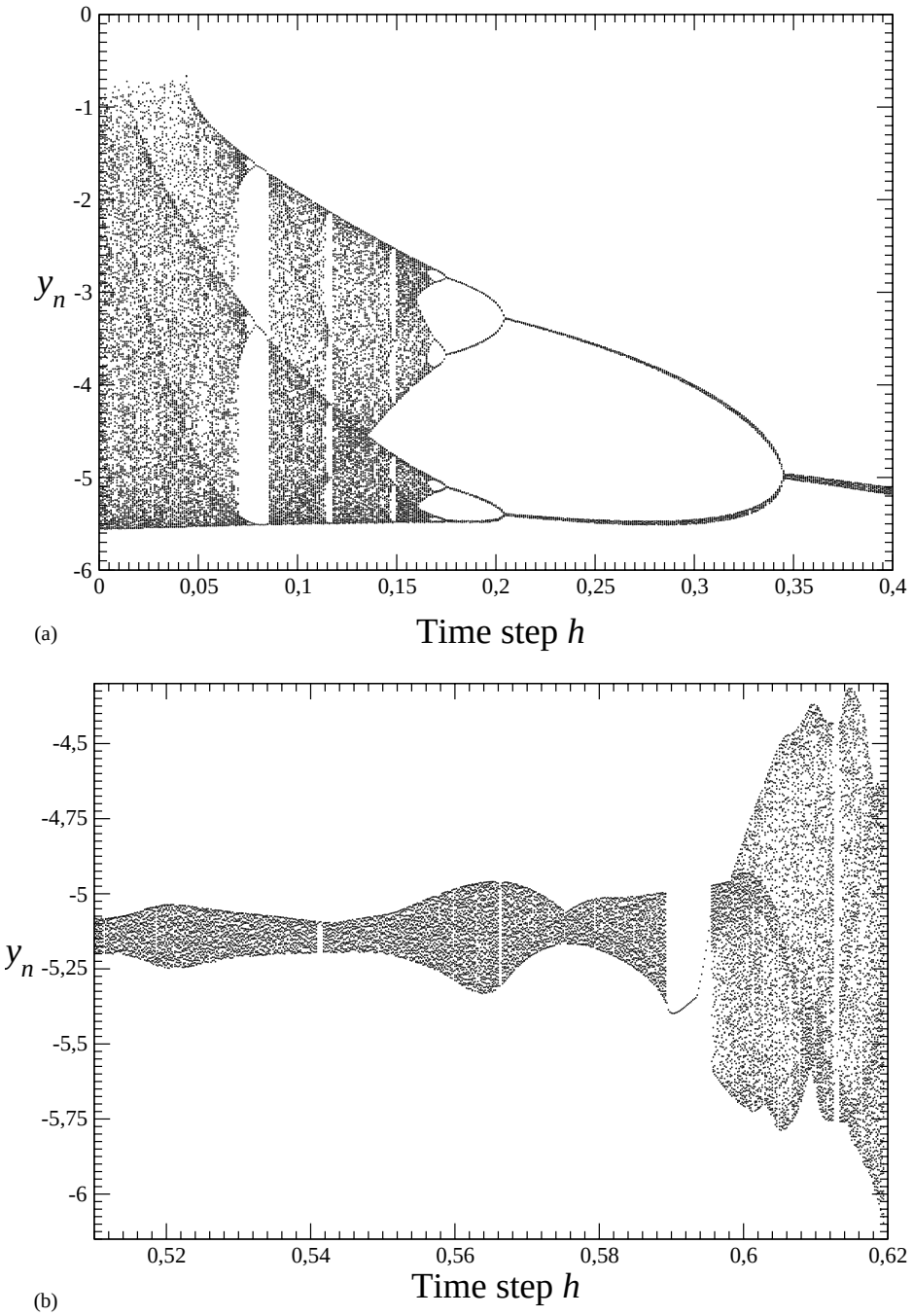

Fig. 7. Bifurcation diagram vs. the time step h for the optimized discrete model (16) with the functions φ_i given in relations (18) and (19). Numerical instabilities occur when the discretization time step is greater than Nyquist's criterion (b).

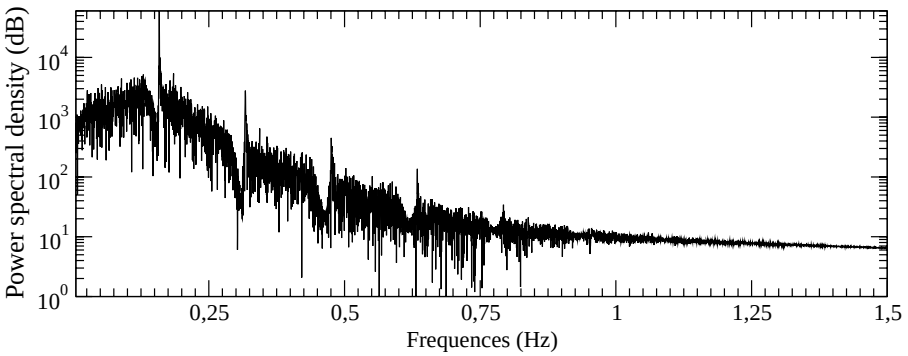

Fig. 8. Fourier spectrum of the Rössler system with $(a, b, c) = (0.432, 2, 4)$. The main frequency f_0 is equal to 0.1587 Hz which corresponds to a pseudo-period equal to 6.3 s. The highest significant frequency $f_{\max} \approx 1.0$ Hz.

"backwards". By similarity it is meant that both models undergo the same sequence of bifurcations. As far as the bifurcations are concerned, the increase of h has a similar effect as the decrease of a. This may be understood by replacing x_{k+1} in second equation of system (16) by the first equation of this system: we thus obtain

$$y_{k+1} = [1 + \varphi_2(a - \varphi_1)]y_k + \varphi_2 x_k - \varphi_1\varphi_2 z_k, \tag{20}$$

where in the term $[1 + \varphi_2(a - \varphi_1)]y_k$, $\varphi_1 = h$ tends to balance the effect of parameter a. The bifurcation diagram (Fig. 7) reveals that the solutions of the discretized version of the Rössler system have clear counterpart solutions in the continuous system for appropriate values of the bifurcation parameters. Note that when $h \in]0, 0.05]$, very few bifurcations are observed and, consequently, the dependence to the solution of the discrete model (16) on the time step size h is very weak. This model is therefore very robust against increase of the time step h.

The pseudo-period of the original Rössler system is 6.3 s as given by the main frequency $f_0 = 0.1587$ Hz (Fig. 8). The largest significant frequency which may be seen in the power spectrum is $f_{\max} \approx 1$ Hz. According to Nyquist's criterion, the sampling frequency should be greater than $2f_{\max}$, that is greater than 2 Hz. At lower sampling rates there would be aliasing of spectra. Such a threshold corresponds to a sampling time $\Delta t \approx 0.5$ s. It is interesting to note that the behaviors, which are no longer topologically equivalent to the solution to the original Rössler system, appear for discretization time step size h greater than the critical sampling time corresponding to Nyquist's criterion.

Indeed, for $h = 0.5$ s, a period-1 limit cycle (Fig. 9a), which is still obviously topologically equivalent to the period-1 limit cycle of the original Rössler system, is observed if the limit cycle is progressively constrained by the heterocline connections between the periodic points of an unstable period-11 orbit (Fig. 9b and c). With $h = 0.589$ s, the limit cycle is shown with the unstable periodic orbit (Fig. 9c) on the continuous Rössler system and, consequently, results from numerical instabilities. When the time step is increased, the limit cycle presents apparent cusps which are actually points of extreme curvature. A similar phenomenon has been observed by Lorenz [22]. Unfortunately, the discrete model is not sufficiently stable to remain stable for a higher discretization time step but we may expect that spurious chaotic behavior would have been observed in such a case. This was observed by Lorenz [22] and in another investigation using another scheme for discretizing another system [26,27].

Note that numerical instabilities appear when the discretization time step h is greater than the Nyquist's criterion. Indeed, the Nyquist criterion is a criterion for the sampling rate of a continuous variable which guarantees that there is no spectra superposition. In other words, this criterion provides an upper value for the time step size at which the time series can be sampled. With greater time steps, some information is lost and the dynamics

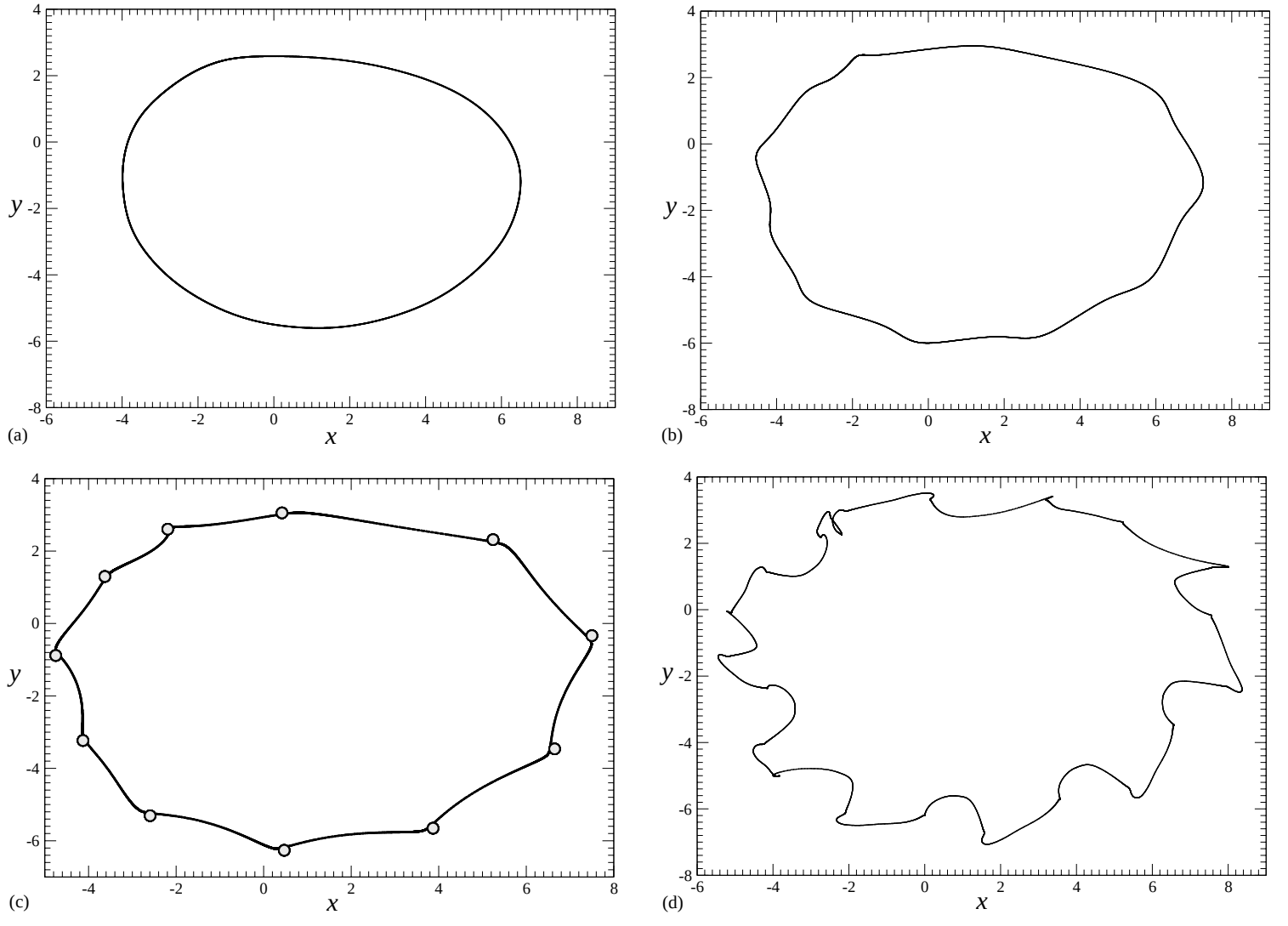

Fig. 9. Solutions to the optimized discrete model of the Rössler system for different values of h. (a) $h = 0.500\,\mathrm{s}$, (b) $h = 0.580\,\mathrm{s}$, (c) $h = 0.589\,\mathrm{s}$, (d) $h = 0.6194\,\mathrm{s}$.

cannot be fully recovered from the measurements. By analogy, we conjecture that when a discretization of a continuous system is built and iterated with a discretization time step size h greater than the Nyquist criterion, the dynamics cannot be recovered without any damage. Consequently, the solutions thus observed are expected not to correspond to a solution to the original differential system, even with a displacement in the parameter space. This is directly related to a comment made by Mickens [24] who stated that numerical instabilities can occur when the finite difference equations do not satisfy some condition that is of importance for the corresponding differential equations. The main time scale of the dynamics is definitely an important characteristic and choosing the time step without any consideration related to this property does not make sense. This means that we obtained difference equations that have good equivalence with the Rössler dynamics, that is, that have a solution that is topologically equivalent to some solution to the Rössler system with a possible displacement in the parameter space.

4. Differential embedding versus delay embedding

In applications, usually only a single time series $\{s(t)\}$ is available to investigate the dynamics. In such cases the first step is to reconstruct the phase space. Two main choices are: using the delay coordinates $\{s(t), s(t+\tau), s(t+2\tau), \dots\}$ or using the derivative coordinates $\{s(t), \dot{s}(t), \ddot{s}(t), \dots\}$. In the first case, a discrete-time model will be attempted [6] while in the second, a continuous-time model has to be estimated [5]. Thus difference or differential equations may be estimated depending on the kind of the embedding chosen. Recent works [10–12] suggest that both approaches are more or less equivalent although rigorous results are still lacking. The structure selection technique implemented for selecting the relevant terms and the dimensionality of the difference equations estimated from the time series [28] usually provides difference equations with a dimensionality greater than the one obtained with differential equations although, in general, with far less terms than the continuous counterpart has. This hampers direct comparison of such mathematical representations. If, on the one hand, the dimensionality of differential models cannot be varied because it is strongly constrained by the embedding dimension [29,30],[1] on the other hand, it is rather natural to find difference equations of orders larger than those of the original systems that produced the data. Therefore, it becomes obvious that it is quite difficult to establish a link between equations working in spaces with different dimension.

In order to show that it is possible to establish an equivalence between a discrete model and a differential one, we will discretize the differential model induced by the y-variable of the Rössler system. Since the equations of the system are known, it is possible to analytically derive the difference model.

Let us assume that the y-variable of the Rössler system is measured. In such a case, the phase space may be reconstructed using the derivative coordinates

$$X = y, \qquad Y = \dot{y}, \qquad Z = \ddot{y}. \tag{21}$$

The reconstructed space is three-dimensional, in agreement with the embedding dimension which can be computed using the false nearest neighbors technique [30]. The derivatives may be expressed analytically using Lie derivatives defined as

$$L_f \Phi(\boldsymbol{x}) = \sum_{k=1}^{3} f_k(\boldsymbol{x}) \frac{\partial \Phi(\boldsymbol{x})}{\partial \boldsymbol{x}_k} \tag{22}$$

and recursively for the higher-order derivatives $L_f^j \Phi(\boldsymbol{x}) = L_f(L_f^{j-1}\Phi(\boldsymbol{x}))$. Here the Rössler system $\dot{\boldsymbol{x}} = \boldsymbol{f}(\boldsymbol{x})$ is observed using $s = \Phi(\boldsymbol{x}) = y$. The function $\Phi : \mathbb{R}^3(x, y, z) \to \mathbb{R}(y)$ is here a smooth function called the

[1] The smallest dimension with which the phase portrait may be represented without self-intersections.

measurement function. Thus, the derivatives are equal to

$$\Theta \equiv \left| \begin{array}{l} X = \Phi(\boldsymbol{x}) = y, \\ Y = L_f \Phi(\boldsymbol{x}) = f_2(\boldsymbol{x}) = x + ay, \\ Z = L_f^2 \Phi(\boldsymbol{x}) = f_1(\boldsymbol{x}) \dfrac{\partial f_2}{\partial x} + f_2(\boldsymbol{x}) \dfrac{\partial f_2}{\partial y} + f_3(\boldsymbol{x}) \dfrac{\partial f_2}{\partial z} = ax + (a^2 - 1)y - z. \end{array} \right. \tag{23}$$

Note that this coordinate transformation $\Theta : \mathbb{R}^3(x, y, z) \to \mathbb{R}^3(X, Y, Z)$ defines a diffeomorphism between the original phase space $\mathbb{R}^3(x, y, z)$ and the differential space $\mathbb{R}^3(X, Y, Z)$ spanned by the successive derivatives of y.

A general form for the differential model induced by the y-variable of the Rössler system reads as

$$\dot{X} = Y, \qquad \dot{Y} = Z, \qquad \dot{Z} = F(X, Y, Z) = L_f^3 \Phi(\boldsymbol{x}), \tag{24}$$

where $F(X, Y, Z)$ is the model function which has to be estimated [5]. In our case, since we know the equations of the original system, this function can be computed analytically. To express the function $F(X, Y, Z)$ in terms of derivative coordinates, the coordinate transformation $\Theta : \mathbb{R}^3(x, y, z) \to \mathbb{R}^3(X, Y, Z)$ given by relation (23) has to be inverted:

$$\Theta^{-1} \equiv \left| \begin{array}{l} x = -aX + Y, \\ y = X, \\ z = -X + aY - Z. \end{array} \right. \tag{25}$$

Thus, the model function reads as [31]

$$F(X, Y, Z) = -b - cX + (ac - 1)Y + (a - c)Z - aX^2 + (a^2 + 1)XY - aXZ - aY^2 + YZ. \tag{26}$$

Such a three-dimensional differential model may be discretized as done for the Rössler system in the previous section. Using the scheme (12), we obtain

$$\begin{aligned} &X_{k+1} = X_k + \varphi_1 Y_k, \qquad Y_{k+1} = Y_k + \varphi_2 Z_k, \\ &Z_{k+1} = \frac{[-b - cX_k + (ac - 1)Y_k + (a - c)Z_k - aX_k^2 + (a^2 + 1)X_k Y_k - aY_k^2]\varphi_3 + Z_k}{1 + \varphi_3(aX_k - Y_k)}, \end{aligned} \tag{27}$$

with $\varphi_1 = \varphi_2 = \varphi_3 = \sin h$. Integration of (27) generates an attractor (Fig. 10a) topologically equivalent to the Rössler system for $h = 0.001$ s. As observed for the various discretizations of the Rössler system, when the discretization time step h is increased, the attractor, which is of the spiral type for small values of h (Fig. 10a), becomes progressively a funnel type attractor (Fig. 10b).

When the discretization time step h is varied, a bifurcation diagram is obtained (Fig. 11a). It is very similar to the diagram of the Rössler system for $a > 0.432$ (Fig. 7b). As we observed for the Rössler system, it is possible to vary the bifurcation parameter to increase the interval over which the discretization time step may be varied. For instance, with $h = 0.101$ s, the a-bifurcation parameter has to be decreased to $a = 0.338$ to recover the spiral attractor with its unimodal map. For this value of a, the discretization time step may be increased up to $h = 0.162$ s (Fig. 11b to compare with Fig. 7a and b) and with $a = 0.200$, h may be increased up to 0.253 s. As observed for the discretization of the Rössler system, the difference equation describing the phase portrait reconstructed using delay coordinates have solution attractors which are topologically equivalent to attractors solution to the Rössler system. Moreover, when the bifurcation parameters are varied, the spiral attractor may be recovered for any value of the discretization time step less than 0.253 s. Note that such a time step h corresponds to roughly 1/25 of the pseudo-period equal to 6.2 s. This is still a very small value since difference equations have been estimated numerically using the technique described in [28] with a time step around to 1.0 s!

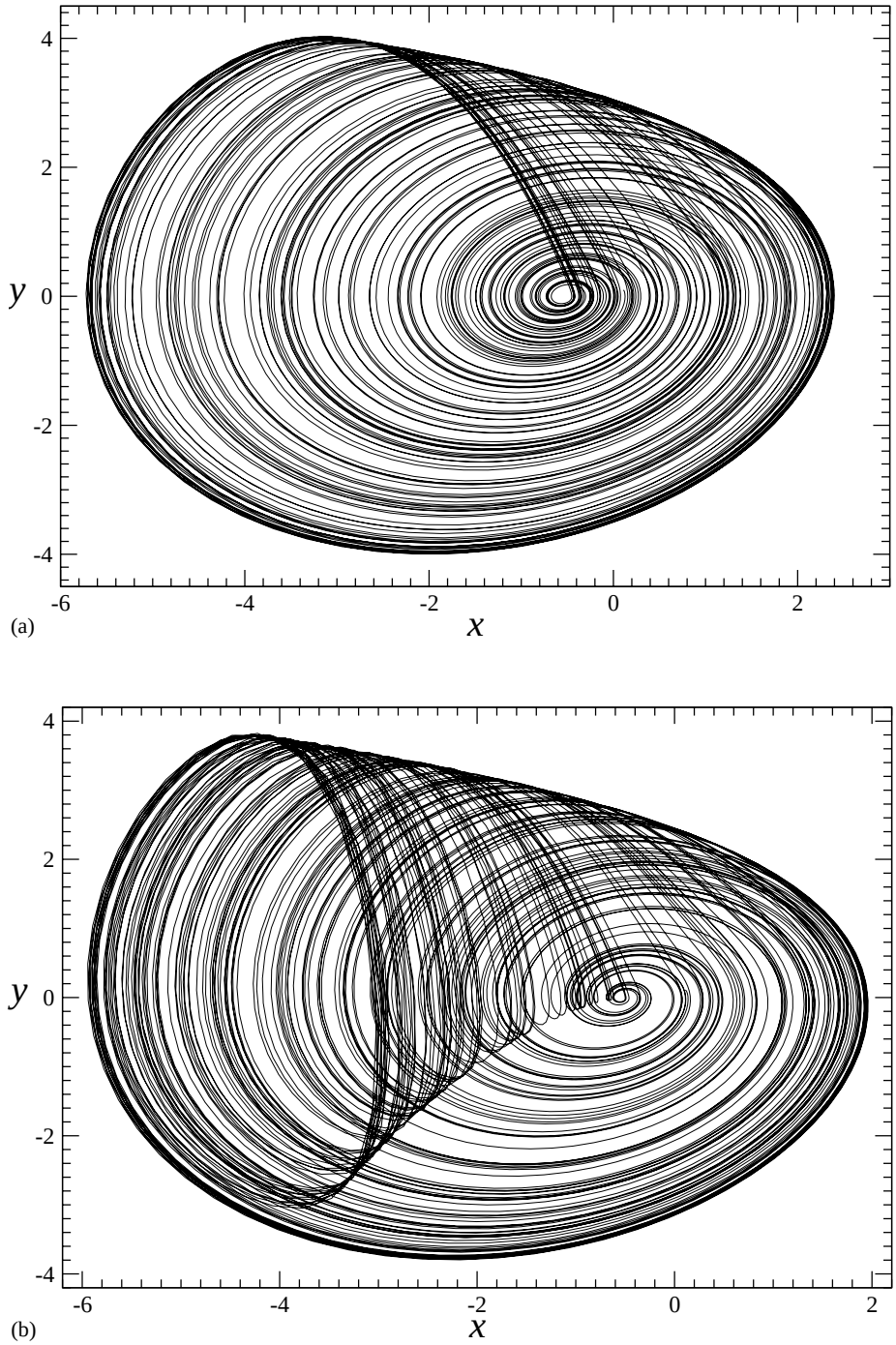

Fig. 10. Attractors of the difference model (27) obtained via discretization using Mickens' scheme, assuming that the observed variable was y. (a) $h = 0.001$ s, (b) $h = 0.101$ s

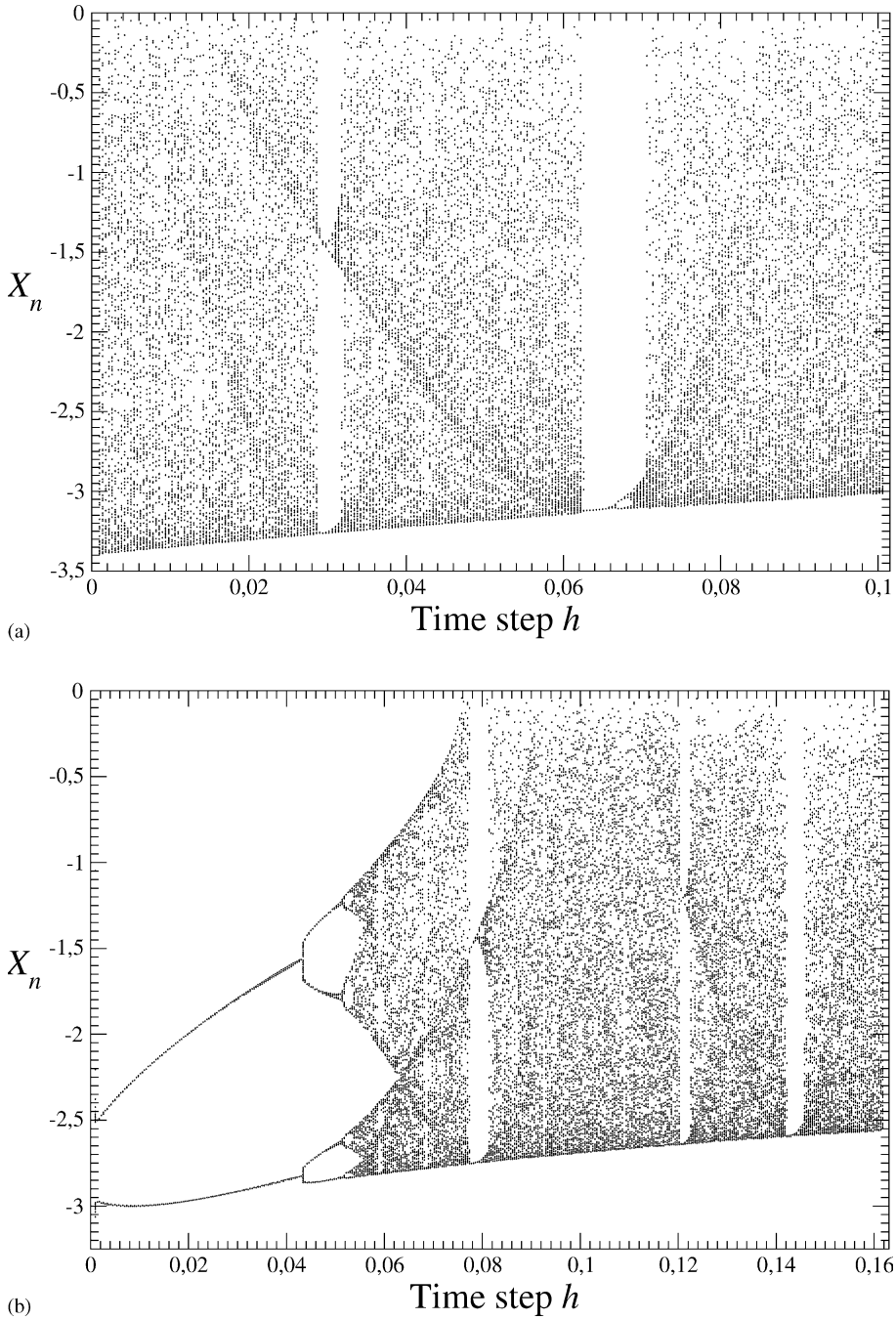

Fig. 11. Bifurcation diagram of the discretization of the differential model induced by the y-variable of the Rössler system for two different values of a. (a) $a = 0.432$, (b) $a = 0.338$.

Applying Mickens' recommendations as done in the previous section. The obtained discrete model reads as

$$\begin{aligned} X_{k+1} &= X_k + \varphi_1 Y_k, \qquad Y_{k+1} = Y_k + \varphi_2 Z_k, \\ Z_{k+1} &= [1 + \varphi_3(Y_{k+1} - aX_{k+1} + a - c)]Z_k \\ &\quad + \varphi_3[-b - cX_{k+1} + (ac-1)Y_{k+1} - aX_kX_{k+1} + (a^2+1)X_{k+1}Y_k - aY_kY_{k+1}], \end{aligned} \tag{28}$$

where $\varphi_1 = \varphi_2 = h$ and

$$\varphi_3 = \frac{1 - \mathrm{e}^{-X_c h}}{X_c}, \tag{29}$$

with $X_c = (c+\sqrt{c^2 - 4ab})/2+a-c$. Unfortunately, this model is less robust against an increase of the discretization time step size since the trajectory settles down onto the inner fixed point for $h = 0.0424$ s. Changing the functions φ_i's does not change this upper value for h.

With this discretization of the differential model induced by the y-variable of the Rössler system, we have an analytical form for the function which can be estimated using discrete polynomial techniques [6,28]. Thus, it is possible to directly compare the model obtained with these theoretical forms. Note that these discretizations are mainly valid when the discretization time step is small enough and, consequently, can be used for comparison when the sampling rate is high enough. Nevertheless, the form of the first discretization is rational while the discrete models to be used are polynomials. We thus have a polynomial approximation of such a rational function. For analytical comparison, (28) would be preferred. It is possible to obtain a discrete polynomial model with a time step h much larger than what is reasonable with the discretization scheme used here. Consequently, such a discretization scheme cannot be applied and more sophisticated ones should be used [26]. Also, since a possible form for the NARMA model induced by the y-variable of the Rössler model can be derived, it is now clearer why the NARMA technique provides more or less the same results than a global modeling technique using derivative coordinates [31]. This is reinforced by the theorem proposed by Mickens [1] which states that an exact finite difference scheme of differential equations always exists. Such an exact discrete model is still to be found for the differential model (26).

5. Conclusion

The problem of the possible equivalence between difference and differential equations has been investigated in the case of the Rössler system. Using nonstandard Mickens' schemes, we showed that the discretizations of the Rössler system have solutions which are topologically equivalent to solutions to the Rössler system with a displacement in the parameter space. This means that varying the time step used in the discretization corresponds to applying a displacement in the parameter space for the original Rössler system. Nevertheless, using Mickens' nonstandard discretization scheme, we found a discretization model very robust under discretization time step increases. In this case, it has been observed that as long as the time step is less than the threshold value associated with the Nyquist criterion, the discrete model has solutions which are topologically equivalent to solutions to the original continuous system with appropriate bifurcation parameter values. This is quite important because this means that there exists a possible discrete counterpart to a set of differential equations as long as the time step does not exceed a value related to the Nyquist's criterion. This is all what we need since when a global model is attempted from a time series, the Nyquist's criterion states that the sampling rate has to be lower than this upper value. Of course, the discrete model proposed here has still to be improved. Unfortunately, there is no general guideline for that and other choices for functions φ and Ψ have to be tried. Nevertheless, this study suggests that a discrete global model of the same dimension as the differential model can be obtained. Such a result already opens new insight for comparing discrete and continuous-time global models.

Acknowledgements

We would like to thank Ronald Mickens for his warm encouragement and helpful remarks to improve this work. C.L. and L.A.A. acknowledge financial support by CNRS and CNPq.

References

[1] R.E. Mickens, Nonstandard Finite Difference Models of Differential Equations, World Scientific, 1994.
[2] K. Inagaki, On the discreteness at the edge of chaos, IPSJ Trans. Math. Model. Appl. 40 (SIG 2(TOM 1)) (1999) 76–81.
[3] S. Elaydi, Is the world evolving discretely? Adv. Appl. Math. 31 (1) (2003) 1–9.
[4] N.H. Packard, J.P. Crutchfield, J.D. Farmer, R.S. Shaw, Geometry from a time series, Phys. Rev. Lett. 45 (9) (1980) 712–716.
[5] G. Gouesbet, C. Letellier, Global vector field reconstruction by using a multivariate polynomial L_2-approximation on nets, Phys. Rev. E 49 (6) (1994) 4955–4972.
[6] I.J. Leontaritis, S.A. Billings, Input–output parametric models for nonlinear systems. Part II. Stochastic nonlinear systems, Int. J. Contr. 41 (2) (1985) 329–344.
[7] R. Brown, N.F. Rul'kov, E.R. Tracy, Modeling and synchronizing chaotic systems from time-series data, Phys. Rev. E 49 (5) (1994) 3784–3800.
[8] F. Takens, Detecting strange attractors in turbulence, Lecture Notes Math. 898 (1981) 366–381.
[9] J.A. Tempkin, J. Yorke, Measurements of a physical process satisfy a difference equation, J. Diff. Eqns. Appl. 8 (1) (2002) 13–24.
[10] C. Letellier, L.A. Aguirre, J. Maquet, A. Aziz-Alaoui, Should all the species of a food chain be counted to investigate the global dynamics? Chaos, Solitons & Fractals 13 (2002) 1099–1113.
[11] C. Letellier, L.A. Aguirre, J. Maquet, B. Lefebvre, Analogy between a 10D model for nonlinear wave–wave interaction in a plasma and the 3D Lorenz dynamics, Physica D 179 (2003) 33–52.
[12] J. Maquet, C. Letellier, L.A. Aguirre, Scalar modeling and analysis of a 3D biochemical reaction model, J. Theor. Biol. 228 (3) (2004) 421–430.
[13] S.A. Billings, L.A. Aguirre, Effects of the sampling time on the dynamics and identification of nonlinear models, Int. J. Bifurc. Chaos 5 (6) (1995) 1541–1556.
[14] P. Liu, S.N. Elaydi, Discrete competitive and cooperative models of Lotka–Volterra type, J. Comput. Anal. Appl. 3 (2001) 53–73.
[15] H. Al-Kahby, F. Dannan, S.N. Elaydi, Non-standard discretization methods for some biological models, in: R.E. Mickens (Ed.), Nonstandard Finite Difference Models of Differential Equations, World Scientific, 2000, pp. 155–188.
[16] R.E. Mickens, Genesis of elementary numerical instabilities in finite-difference models of ordinary differential equations, Proc. Dynam. Syst. Appl. 1 (1994) 251–258.
[17] L.A. Aguirre, S.A. Billings, Dynamical effects of overparametrization in nonlinear models, Physica D 80 (1995) 26–40.
[18] R. Gilmore, Topological analysis of chaotic dynamical systems, Rev. Mod. Phys. 70 (4) (1998) 1455–1529.
[19] O.E. Rössler, An equation for continuous chaos, Phys. Lett. A 57 (5) (1976) 397–398.
[20] J.D. Farmer, J.P. Crutchfield, H. Frœling, N.H. Packard, R.S. Shaw, Power spectra and mixing properties of strange attractors, Ann. NY Acad. Sci. 357 (1980) 453–472.
[21] C. Letellier, P. Dutertre, B. Maheu, Unstable periodic orbits and templates of the Rössler system: toward a systematic topological characterization, Chaos 5 (1) (1995) 271–282.
[22] E.N. Lorenz, Computational chaos—a prelude to computational instability, Physica D 35 (1989) 299.
[23] R.R. Whitehead, N. Mc Donald, A chaotic mapping that displays its own homocline structure, Physica D 13 (1984) 401.
[24] R.E. Mickens, Nonstandard finite difference schemes for differential equations, J. Diff. Eqns. Appl. 8 (9) (2002) 823–947.
[25] L.A. Aguirre, C. Letellier, J. Maquet, Induced bifurcations in the validation of nonlinear dynamical models, Int. J. Bifurc. Chaos 12 (1) (2002) 135–145.
[26] E.M.A.M. Mendes, S.A. Billings, A note on discretization of nonlinear differential equations, Chaos 12 (1) (2002) 66–71.
[27] E.M.A.M. Mendes, C. Letellier, A new discretization scheme for large discretization time step, J. Phys. A 37 (2004) 1203–1218.
[28] L.A. Aguirre, S.A. Billings, Retrieving dynamical invariants from chaotic data using NARMAX models, Int. J. Bifurc. Chaos 5 (2) (1995) 449–474.
[29] H.D.I. Abarbanel, M.B. Kennel, Local false nearest neighbors and dynamical dimensions from observed chaotic data, Phys. Rev. E 47 (5) (1993) 3057–3068.
[30] L. Cao, Practical method for determining the minimum embedding dimension of a scalar time series, Physica D 110 (1/2) (1997) 43–52.
[31] C. Letellier, J. Maquet, L. Le Sceller, G. Gouesbet, L.A. Aguirre, On the non-equivalence of observables in phase space reconstructions from recorded time series, J. Phys. A 31 (1998) 7913–7927.